18th International Symposium on Flow Visualization
Zurich, Switzerland, June 26-29, 2018

VISUALIZING THE SWIM TECHNIQUE OF A PULLER-TYPE MICRO-SWIMMER WITHOUT VISUALIZING THE FLAGELLUM

F. G. Ergin[1,c]

[1]Dantec Dynamics, Tonsbakken 16-18, 2740, Skovlunde, Denmark
[c]Corresponding author: Tel.: +4544578000; Email: gokhan.ergin@dantecdynamics.com

KEYWORDS:
Puller-type microscopic swimmer, Micro Particle Image Velocimetry, Dynamic masking

ABSTRACT: *The locomotion mechanism of Euglena Gracilis is investigated using microscopic shadow imaging and Micro Particle Image Velocimetry (μPIV). Three distinct locomotion modes were observed; translation, spin and left/right turn. Since the flagellum was not possible to image, the strokes were identified by evaluating the flow field around the protist. The flow field information is obtained using a phase-separated PIV evaluation, which uses of a histogram-thresholding based dynamic masking approach. The temporal resolution of the experiment was sufficient to identify the sequence of translation and spin, and the stroke-pulling frequency. The results indicate that the organism has a complex locomotion technique that allows the change of direction, change of axial orientation and propulsion.*

1 INTRODUCTION

Euglena gracilis (E. gracilis) is a protist microorganism that populates in fresh water habitats and sustains life by collecting solar energy by photosynthesis using chloroplasts. Its body length without the flagellum can vary between 20 μm and 100 μm. The optimum light level for chloroplasts is around 30 W/m2, and therefore E. gracilis is known to adjust its depth in water in order to find this optimum light condition [1]. This necessitates the photo detection, sense of gravity and locomotion, which are vital functionalities for E. gracilis' survival. The basic aerotaxis (moving towards oxygen), gravitaxis (moving up and down) and phototaxis (moving towards or away from light) behaviour is explained in detail in Ref. 1, where underlying chemistry necessary for locomotion is provided. In the next paragraph we provide the relevant points of E. gracilis locomotion behavior from Ref. 1, which consists of thee modes; forward translation, spin along long axis and the euglenoid movement.
The flagellum is actively used during translation and spin. In fact, E. gracilis has two anterior trailing flagella, but only the long, protruding one is the main source of forward propulsion (Fig.1c). The flagellum is located at one end close to the photoreceptor and the reservoir, whereas the cell nucleus is centrally located in its body. The flagellar beats could be in the form of pulling strokes that results in a forward translation, or rotational strokes that results the E. gracilis to spin around its long axis. In this work we are only interested in resolving the flagellar beats that are in the form of pulling strokes, i.e. stroke-pulling frequency. The rotational movement of E. gracilis is often associated with phototaxis, where the organism senses the light propagation direction: This is accomplished by spin swimming where varying amplitudes of light is registered on the photoreceptor due to changing incidence angle of the light rays. This would normally create two maxima per spin, due to a dichroitic orientation of the photoreceptor molecules in the stigma (eye spot, Fig. 1a) the light direction is determined unambiguously. The final locomotion mode is the euglenoid movement, which can be described by the bending and stretching of the organism either in order to change direction or move forward like a snail.

The euglenoid movement is often attributed to the pellicular stripes (Fig. 1b and 1c), microtubules that can slide on each other, which gives the extreme flexibility to E. gracilis. [1]
Recent SEM pictures of the E. gracilis reveal that the pellicular stripes are oriented resembling the threads of a left-hand screw (Fig. 1b and 1c), a schematic of which is given in Fig. 1d. The pellicular stripes are oriented at approximately 45° angle with respect to its long axis. This is determined by two separate image rotations applied on Fig. 1c, first an 18° counter-clockwise (ccw) rotation to align the long axis with the vertical, and second a 63° ccw rotation to align the stripes with the horizontal. The difference is the thread angle at the equatorial positions, which changes to 90° close to the anterior tip.

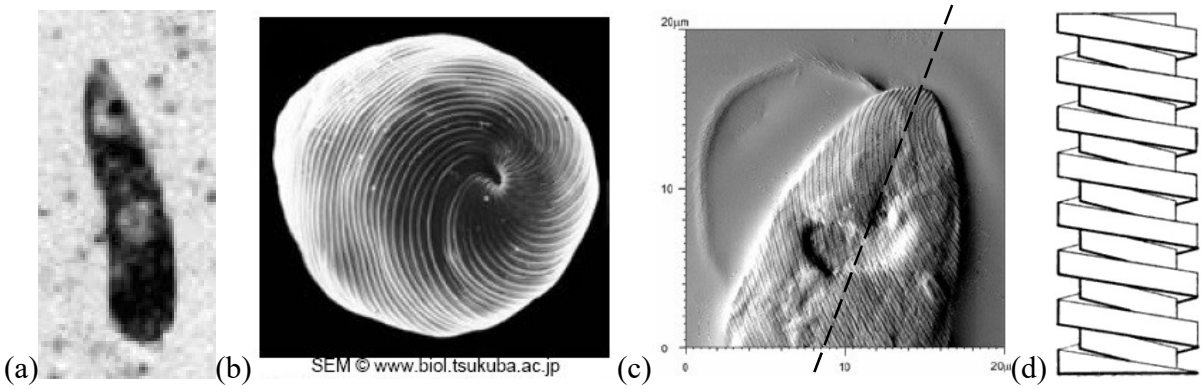

Fig. 1 (a) Picture of the 48 µm-tall, 10 µm-diameter E. gracilis under investigation (b) SEM image of the threaded screw like surface texture. Printed with permission. © Isao INOUYE, Institute of Biological Sciences, University of Tsukuba (c) AFM image of the threaded screw like surface texture. Image adapted from Fig. 4 in Ref. [2]. Reproduced with permission. Dashed line in (c) is the approximate location of the long axis. (d) Schematic of a left handed mechanical screw. Image credits: Wikipedia commons.

Although much is known about *E. gracilis*' locomotion behaviour, a quantitative evaluation of hydrodynamics during locomotion has not been reported. In this study, the aim is to quantify these three modes (translation, spin and turns) using microscopic imaging, dynamic masking and Micro Particle Image Velocimetry (µPIV). In the following sections the average linear swim speed, spin rate, hydrodynamics of the stroke mechanism, sequence of the swimming modes and the relation between threaded screw like surface texture and the spin mode are investigated.

2 METHODS

2.1 Experimental Setup

The experiments were performed in still water and a cold light source ensured that there was no background flow due to convection currents. The flow field around E. gracilis is measured using time-resolved MicroPIV. The use of particle imaging and tracking techniques for the investigation of flow fields of motile organisms is not new; some recent examples can be found in References [3-8]. The MicroPIV system is manufactured by Dantec Dynamics A/S (Skovlunde, Denmark), and is explained in detail in Ref. [9]. Briefly, the components include an inverted fluorescence Microscope, a sensitive CMOS detector, a synchronization device, and a pulsed LED illumination system. In biological flows, high-power pulsed laser illumination is not preferred as this can disable the organism. For this reason, a lower-power, green LED-based pulsed illumination was used in transmission mode. The green colour simulates a natural environment, such as a fresh water pond surface where E. gracilis flourish. 1 µm-

diameter seeding particles were introduced in small quantities until a sufficient seeding density for PIV was achieved. The seeding density was kept at a low level in order to avoid possible changes in the normal swimming behaviour. The particle images were recorded at a frame rate of 12.5 fps (constant time difference of 80ms), at a resolution of 1280x800 pixels. The images were acquired using a 40x magnification objective, producing a 0.4 mm x 0.64mm-wide field of view (FoV) and 1 µm-thick field depth. The small field depth ensures that the measured displacements are planar. Later a smaller region of interest is extracted with a resolution of 323x529 pixels, corresponding to 162 µm x 265 µm in the object space. Since the FoV was really small (~0,25mm^2), it was often necessary to wait until an organism swims through the FoV with the measurement system is in operation. The raw images were stored in a ring buffer and the acquisition is stopped manually after the organism passed through the FoV.

2.2 Dynamic Masking

Before PIV evaluation, the image of *E. gracilis* was removed from the flow field using dynamic masking [9-11]. This is necessary because the movements of the organism are not related to the fluid motion in the vicinity of *E. gracilis*. For example during the stroke, the fluid upstream is pulled towards *E. Gracilis* (downwards), while it is swimming in the other direction (upwards). If not removed, the moving features on *E. gracilis* image (stigma, nucleus etc.) contributes to the cross correlation function during the velocity calculation and introduces an error in of the flow field. This is well illustrated in Fig. 6 in Ref. [11]. Additionally the details of the image pre-processing steps used to achieve the dynamic mask are provided [11]. Briefly, first a pixel inversion is performed to work with positive particle images instead of particle shadows. Second, a background subtraction is performed using the minimum pixel value found in the original ensemble. Third, a histogram-thresholding based binary dynamic mask ensemble is produced using the images in the second step and finally image masking is performed by multiplication of the binary mask with the background-removed images. The dynamic mask captures the position and the shape of Euglena gracilis in a successful fashion (Figure 2).

2.3 Velocimetry

Details of the velocity calculations are provided in Ref. [11]. Briefly, an adaptive PIV algorithm is used, which is an advanced particle displacement estimator implemented in DynamicStudio (Dantec Dynamics, Skovlunde, Denmark). The calculation is a cross-correlation based, adaptive and iterative procedure with vector validation and deforming windows. For the current case, interrogation windows of 32x32 pixel are used with 75% overlap. Window deformation is performed by adapting the interrogation area shape to velocity gradients. Several passes can be made to further shift & deform the windows to minimize the in-plane particle dropout. This procedure is repeated until a convergence limit in pixels or a maximum number of iterations is reached. Then a 2D Gaussian fit is performed on the highest correlation peak to calculate the displacement field with sub pixel accuracy. Between passes, spurious vectors are identified and replaced with a number of validation schemes. The sub pixel positioning accuracy of the Adaptive PIV algorithm is reported as 0.06 pixels with 95% confidence [12]. The 0.06 pixels correspond to a 27.5nm displacement in the object space, and the velocity uncertainty is estimated as 0.34 µm/s. An average filter in a 5x5 neighborhood and vector masking is applied after Adaptive PIV computations.

3 RESULTS

The swimming modes of the experiments are extracted from a single trajectory of a single organism performing 4 strokes and 4 spins where 2 right turns and 2 left turns were executed. In fact, each stroke is followed by a spin. *E. gracilis* meanders upwards through filtered water; covering a net distance of approximately 256 µm and a gross displacement of 292 µm in 6.56s, yielding an average swim speed of ~44.5 µm/s. The net to gross displacement ratio, NGDR, for this track is calculated as 0.88. The shape of the organism at equidistant time steps is shown in Fig. 2.

Fig. 2 Position of E. gracilis recorded every 0.96s found by the dynamic mask.

3.1 Spin

The first locomotion mode observed during the experiments is the spinning motion (Fig. 3). The motion can be observed by tracking the position of the stigma relative to the main axis. In Figure 2a, the stigma is located on the top right of the organism and moves towards the center and further to the left in time. In time, the stigma becomes invisible as it moves below the organism. The swimmer is observed to spin in the same direction in all four spins; counter clockwise looking from the trailing edge. There is a second motion in Fig. 3, which can be observed by tracking the organism within the frame: the organism glides forward as it spins towards the left. This is important, as it resembles the motion of a left-handed mechanical screw as in Fig. 1d.

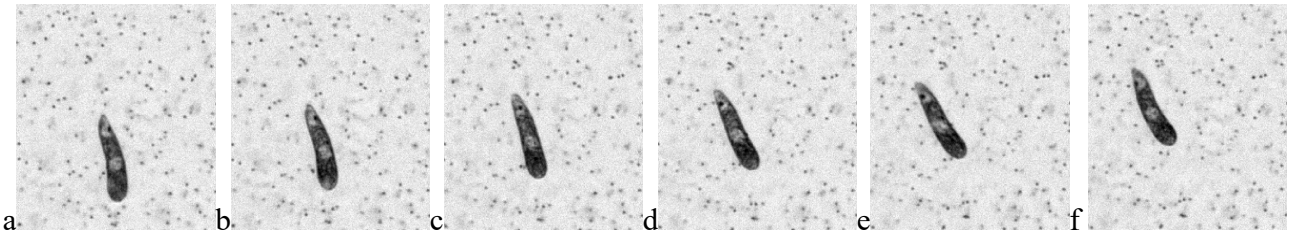

Fig. 3 Spinning motion of E. gracilis at t=2s (a), t=2.16s(b), t=2.32s(c), t=2.48s(d), t=2.64s(e), and t=2.8s(f).

It is found that E. gracilis has a rather steady spin rate, and it completes half a revolution in 0.8s, and thus spin rate is 0.625 revs/s. The linear translation is computed by subtracting the tip position in Fig. 3a and 3f: E. gracilis moves 32.65 µm forward in 0.8s, resulting in an instantaneous linear speed of 40.8 µm/s, and this is consistent with the average swim speed.

3.2 Stroke

The flow field around E. gracilis is measured using µPIV and dynamic masking. Close ups of the flow field during several stroke instances are shown in Fig. 4. In these figures, vectors represent the u and v components of the flow field and colors represent the magnitude of local velocity, where blue areas represent stagnant flow regions. The stroke is observed first at t=1.92s, and then at t=3.52s, 4.32s and 5.12s, exactly every 0.8s (corresponding to 1.25Hz). The time difference between the 1.92s and 3.52s is 1.6s, corresponding to half of 1.25Hz. This is in very good agreement with the findings of Ref. [13] that report a cell body rotation frequency of 1.2Hz for a single E. gracilis using light scattering experiments (Fig. 3 in Ref. [13]). Ref. [14] reports 50% higher value for cell body rotation frequency: 1.8Hz. For a population of E. gracilis the frequency band widens approximately 0.5Hz (Fig. 4a in Ref. [13]). The term cell body rotation frequency used by Ref. [13] is an equivalent term to the stroke-pulling frequency used in this work, because it will be shown in the next section that each stroke is followed by a spin. The stroke-pulling frequency should not be confused with the faster flagellum beating frequency, which is reported between 30 Hz - 40 Hz in the literature for E. gracilis [13-16].

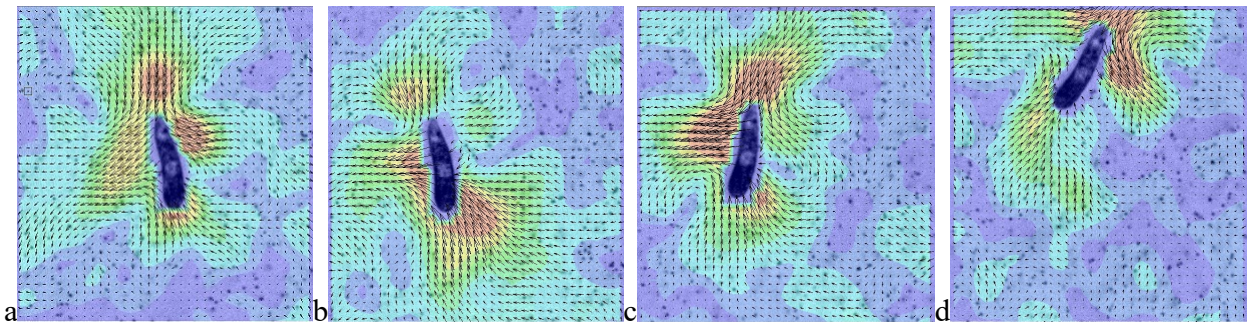

Fig. 4 E. gracilis pulling strokes at t=1.92s, 3.52s, 4.32s and 5.12s

The flow field around E. gracilis reveals that the fluid is drawn towards the organism upstream and downstream, and fluid is expelled from the organism on the sides (Fig. 4). The upstream flow field is produced by the flagellum pulling a stroke, the main source of propulsion. The downstream flow field can be explained as the wake in the aft of the swimmer. Due to continuity around the organism, the fluid is expelled outwards from the sides. This type of flow field produces four stagnant flow regions, one at each corner of the organism, i.e. due Southwest, Southeast, Northwest and Northeast of the organism.

3.3 Sequence of locomotion modes: stroke and spin

Once the two major swimming modes are established, it is interesting to know the sequence of events: in other words, whether the stroke and spin are simultaneous or whether one is after the other. Figure 5 shows the flow field around E. gracilis during a stroke followed by a spin where flow fields are shown with equal time spacing of 240ms. In Fig. 5a, E. gracilis is at the beginning of pulling a stroke, where the fluid upstream of E. gracilis has just started moving towards the organism. In Fig. 5b, the stroke is

close to its maximum power where the pulled (upstream) and expelled (on each side) fluid velocities reach to maximum values. In Fig. 5c, the stroke is slowing down and comes to an end in Fig. 5d, when E. gracilis starts its spin as the stigma begins moving towards the left. The spinning motion continues in Fig. 5e and 5f. Since the flagellum is not visible in the raw images it is not possible to clarify whether E. gracilis actively rotates the flagellum in the clockwise (cw) direction in order to spin in the ccw direction, or it just passively lets the fluid friction along the pellicular stripes to put itself in a spiral motion.

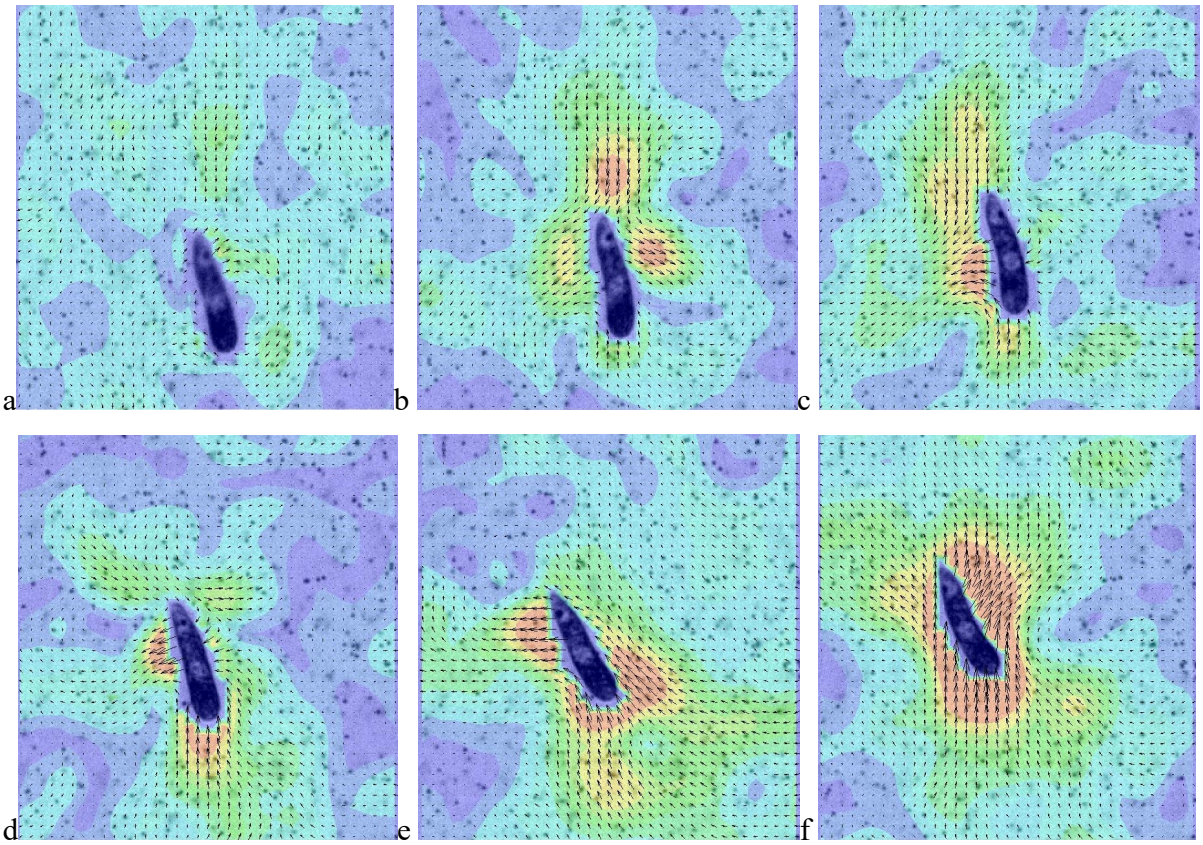

Fig. 5 E. gracilis during a stroke at t=1.6s, 1.84s, 2.08s followed by a spin at t=2.32s, 2.56s, 2.8s.

3.4 Left and Right Turns

During the experiments E. gracilis executes two left turns (these are shown in Fig. 6a and 6b) and two right turns (these are shown in Fig. 6c and 6d). An important observation is made from the hydrodynamics of the flow field during turns: when E. gracilis is turning left, it creates vortex on its left (Fig. 6a and 6b), and when it is turning right, it creates a vortex on its right (Fig. 6c and 6d). The vortex core is located closer to the trailing edge of E. gracilis at a distance of 1 to 3 diameters from the organism.

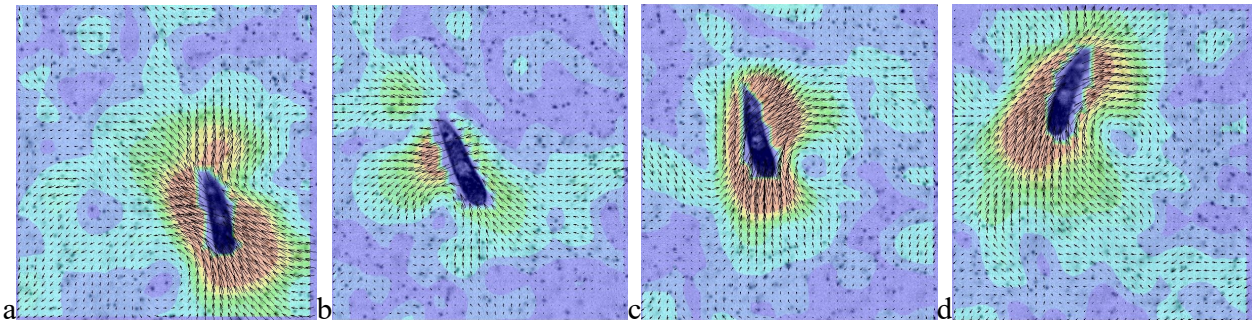

Fig. 6 E. gracilis performing left turns (a and b) and right turns (c and d).

The creation of these vortices can be explained by the local pressure distribution around E. gracilis. First of all since E. gracilis is in forward motion, there is normally a constant suction pressure on its tail. During a left turn, the fluid on the left is being pushed leftwards, and therefore a positive pressure on the left is formed (Fig. 6a and 6b). The continuity equation must be satisfied and the fluid under suction pressure in the wake of E. gracilis is replaced by the fluid under positive pressure on its left. This forces the fluid to rotate and form a ccw vortex on the left. The opposite happens during a right turn; a positive pressure is formed on the right-hand side and this fluid replaces the fluid in the wake. This forces the fluid to rotate and form a cw vortex on the right. Due to the presence of a vortex during turns, the flow disturbances created during turns can extend up to 5 to 7 diameters from the organism which increases the risk of detection by predators. It is not yet clear how the E. gracilis mechanically initiates each turn, but there are four possibilities: (a) bending its body in the direction of the turn (Fig. 6a, 6c and 6d), (b) using the flagellum in a side-pushing stroke, (c) using a buckling instability of the hook and or (d) a combination of these three. For the case in (c), Ref. [17] suggests that uniflagellate bacteria with posterior-attached flagella ("fluid pushers") exploit a buckling instability of the hook in order to change direction during forward swimming. It is not clear whether a similar mechanism is involved here since the forward swim is achieved by pulling strokes in the case of E. gracilis, where the flagellum is attached in the anterior.

4 CONCLUSIONS AND OUTLOOK

The quantitative experimental visualization results provide significant insight into E. gracilis locomotion hydrodynamics. First and foremost, the sequence of spin and stroke mechanisms is established. It is interesting that the E. gracilis pulls a stroke followed by a spin, which is somewhat similar to the human freestyle swim technique. How the organism initiates the spin is still not very clear; passively due to helical pellicular stripes, actively using the flagellum or a combination of both. Second, the angular orientation and handedness (twist direction) of the pellicular stripes is established. There are sufficient reasons to think that the left-handed helical pellicular stripes either assist or sustain the spinning motion of E. gracilis. Third, average swim speed and the spin rate, are calculated. Using the average swim speed, the average swim power can be estimated. This is closely related to the average power used in the flagellum during strokes during forward translation. This could be a first step for estimating the locomotion cost for E. gracilis in search for nutrient zones in darkness, move towards light in low light conditions or move away from light in excessive light conditions. Fourth, the hydrodynamics related to stroke and left / right turns are established. The results indicate that during stroke and turns the hydrodynamic flow disturbances can reach as much as 5-7 diameters, and this increases the risk of detection by predators. Additionally, vortices are introduced in the flow during

strokes and turns, which enhance mixing in the vicinity of E. gracilis. As mentioned above, there are a number of unanswered questions that can be resolved by imaging the flagellum – with a higher frequency MicroPIV system: (i) whether flagellum plays a role during spin initiation, (ii) higher-frequency flagellar beating frequency, and (iii) how the flagellum is used during turns. Future work aims to utilize a fluorescence-staining technique reported in Ref. [18] in the real-time imaging of the flagellum during MicroPIV experiments. Since the flagellum can rotate freely in 3D space, future experiments are planned to measure the third velocity component using a high-speed Stereoscopic MicroPIV system.

5 ACKNOWLEDGMENTS

The author wishes to thank Dr. Giovanni Noselli for providing the culture for Euglena gracilis, and Dr. Lalith Wickramarathna for many helpful comments and suggestions.

References

[1] Häder DP, Faddoul J, Lebert M, Richter P, Schuster M, Richter R, Strauch SM and Daiker V. Investigation of Gravitaxis and Phototaxis in Euglena gracilis. *Advances in Life Sciences* Chapter 4, 117-131, 2011

[2] Gruenberger C, Ritter R, Aumayr F, Stachelberger H and Gebeshuber IC. Algal Biophysics: Euglena gracilis Investigated by Atomic Force Microscopy. *Materials Science Forum* Vol. 555, pp. 411-416, 2007.

[3] Nielsen LT and Kiørboe T. Feeding currents facilitate a mixotrophic way of life. *The ISME Journal*, 1–11, 2015

[4] Kiørboe T, Jiang H, Gonçalves RJ, Nielsen LT and Wadhwa N. Flow disturbances generated by feeding and swimming zooplankton. *PNAS*, vol. 111, no. 32, 11738–11743, 2014.

[5] Wadhwa N, Andersen A and Kiørboe T. Hydrodynamics and energetics of jumping copepod nauplii and copepodids. *J. of Exp. Biol.* 217, 3085-3094 doi:10.1242/jeb.105676, 2014.

[6] Roper M, Dayel MJ, Pepper RE and Koehl MAR. Cooperatively Generated Stresslet Flows Supply Fresh Fluid to Multicellular Choanoflagellate Colonies. *PRL* 110, 228104, 2013.

[7] Pepper RE, Roper M, Ryu S, Matsudaira P and Stone HA. Nearby boundaries create eddies near microscopic filter Feeders. *J. R. Soc. Interface* 7, 851-862, 2010.

[8] Guasto JS, Johnson KA, and Gollub JP. Oscillatory Flows Induced by Microorganisms Swimming in Two Dimensions. *PRL* 105, 168102, 2010

[9] Ergin FG. Flow field measurements during microorganism locomotion using MicroPIV and dynamic masking. *Proc. 11th Int. Symp. on PIV.* Santa Barbara, California, September 14-16, 2015

[10] Ergin FG. On dynamic masking of time resolved PIV data. *Proc. of 10th European Fluid Mechanics Conference (EUROMECH) EFMC10* Copenhagen, September 15-18, 2014.

[11] Ergin FG. Dynamic masking techniques for particle image velocimetry. *J. of Thermal Science and Technology*,Vol 37, 2, pp. 61-74. ISSN 1300-3615, 2017.

[12] Ergin FG, Watz BB, Erglis K and Cebers A. Time-resolved velocity measurements in a magnetic micromixer. *Exp. Therm. Flu. Sci.* 67, pp. 6-13, 2015.

[13] Angelini F, Ascoli C, Frediani C and Petracchi D. Transient Photoresponses of a Phototactic Microorganism, Haematococcus Pluvialis, Revealed by Light Scattering. *Biophys. J. Biophysical Society* Vol. 50 pp.929-936, 1986.

[14] Ascoli C, Barbi M, Frediani C and Mure A. Measurements of Euglena motion parameters by laser light scattering. *Biophys. J.* 211:585-599, 1978.

[15] Ascoli C and Frediani C. Quasi-elastic light scattering in the measurement of the motion of flagellated algae. *Light Scattering in Liquids and Macromolecular Solutions*. Plenum Publishing Corp., London. 183-198, 1980.

[16] Chen SH and Hallett FR. Determination of motile behavior of prokaryiotic and eukaryotic cells by quasi-elastic light scattering. *Q. Rev. Biophys*. 15:131-222, 1982.

[17] Son K, Guasto JS and Stocker R. Bacteria can exploit a flagellar buckling instability to change direction. *Nature physics*, 9, 494-498, 2013.

[18] Turner L, Ryu WS and Berg HC. Real-Time Imaging of Fluorescent Flagellar Filaments. *J. Bacteriol*. Vol. 182, No. 10, p. 2793–2801, 2000.

Copyright Statement

The authors confirm that they, and/or their company or institution, hold copyright on all the original material included in their paper. They also confirm they have obtained permission, from the copyright holder of any third-party material included in their paper, to publish it as part of their paper. The authors grant full permission for the publication and distribution of their paper as part of the ISFV18 proceedings or as individual off-prints from the proceedings.